

## A new estimate of the CaCO<sub>3</sub> to organic carbon export ratio

J. L. Sarmiento, J. Dunne, A. Gnanadesikan,<sup>1</sup> R. M. Key, K. Matsumoto, and R. Slater

Atmospheric and Oceanic Sciences Program, Princeton University, Princeton, New Jersey, USA

Received 19 April 2002; revised 10 July 2002; accepted 24 July 2002; published 3 December 2002.

[1] We use an ocean biogeochemical-transport box model of the top 100 m of the water column to estimate the CaCO<sub>3</sub> to organic carbon export ratio from observations of the vertical gradients of potential alkalinity and nitrate. We find a global average molar export ratio of  $0.06 \pm 0.03$ . This is substantially smaller than earlier estimates of 0.25 on which a majority of ocean biogeochemical models had based their parameterization of CaCO<sub>3</sub> production. Contrary to the pattern of coccolithophore blooms determined from satellite observations, which show high latitude predominance, we find maximum export ratios in the equatorial region and generally smaller ratios in the subtropical and subpolar gyres. Our results suggest a dominant contribution to global calcification by low-latitude nonbloom forming coccolithophores or other organisms such as foraminifera and pteropods.

*INDEX TERMS:* 4805 Oceanography: Biological and Chemical: Biogeochemical cycles (1615); 4806 Oceanography: Biological and Chemical: Carbon cycling; 4842 Oceanography: Biological and Chemical: Modeling; 4845 Oceanography: Biological and Chemical: Nutrients and nutrient cycling;

*KEYWORDS:* calcium carbonate, organic carbon, export ratio, ocean biogeochemistry

**Citation:** Sarmiento, J. L., J. Dunne, A. Gnanadesikan, R. M. Key, K. Matsumoto, and R. Slater, A new estimate of the CaCO<sub>3</sub> to organic carbon export ratio, *Global Biogeochem. Cycles*, 16(4), 1107, doi:10.1029/2002GB001919, 2002.

### 1. Introduction

[2] Ocean biogeochemistry models generally parameterize CaCO<sub>3</sub> production in such a way as to fit a particular estimate of the CaCO<sub>3</sub> to organic carbon export ratio. However, observationally based estimates of the global CaCO<sub>3</sub> to organic carbon export ratio vary by a factor 5 from a high of 0.25 to a low of 0.05 to 0.08 (see Table 1). Most model simulations have specified export ratios at the higher end of the observationally based range estimates (0.15 to 0.25, see Table 1 [e.g., Archer *et al.*, 2000; Bacastow and Maier-Reimer, 1990; Maier-Reimer, 1993; and Aumont, 1998]), but two recent model studies (Yamanaka and Tajika [1996] and R. G. Najjar and J. C. Orr, Design of OCMIP-2 simulations of chlorofluorocarbons, the solubility pump and common biogeochemistry, 1998; available from the World Wide Web at <http://www.ipsl.jussieu.fr/OCMIP/>) used estimates at the low end of the range.

[3] The choice of ratio has a significant impact on the scope for changes in the oceanic CaCO<sub>3</sub> cycle to modify the distribution of CO<sub>2</sub> between the atmosphere and ocean. In a recent study, Matsumoto *et al.* [2002] explored how the sensitivity of atmospheric carbon dioxide to changes in the export ratio depends on the assumed starting value for the export ratio. The motivation for their study was the proposal by Archer [1996] and Archer *et al.* [2000] that a

decline in the export ratio of CaCO<sub>3</sub> to organic carbon may have contributed to the reduction in atmospheric CO<sub>2</sub> that occurred during the last ice age. The magnitude of the response of atmospheric CO<sub>2</sub> to a change in the export ratio depends on whether or not the response of the CaCO<sub>3</sub> cycle in ocean sediments is included. The sediment CaCO<sub>3</sub> cycle takes thousands of years to adjust to a change in the export ratio. Thus, its contribution can be ignored on century timescales (the closed system response) but not on millennial timescales (the open system response). In their study, Matsumoto *et al.* [2002] show that the open system response of atmospheric CO<sub>2</sub> to the mechanism proposed by Archer and Maier-Reimer [1994], Archer [1996], and Archer *et al.* [2000] depends only on the fractional change in the export ratio, not on the absolute magnitude of this change. For example, a 40% reduction in the export ratio from 0.25 to 0.15 (Case A) or from 0.05 to 0.03 (Case B) will both give approximately the same magnitude of response in atmospheric carbon dioxide on a millennial timescale. However, the short timescale closed system response is almost linearly dependent on the change in the export ratio. Thus, on a short timescale, the higher the assumed present CaCO<sub>3</sub> export ratio is, the more leeway there is for changes in the export ratio to influence atmospheric CO<sub>2</sub>. In the example above, the high export ratio model, Case A, will have about five times the capacity of the low export ratio model, Case B, for reductions in the oceanic CaCO<sub>3</sub> cycle to draw down atmospheric CO<sub>2</sub>.

[4] The higher estimates of the export ratio used in earlier models can generally be traced back to a misinterpretation of the studies of Li *et al.* [1969] and Broecker [1971]. These

<sup>1</sup>Now at Geophysical Fluid Dynamics Laboratory, NOAA, Princeton, New Jersey, USA.

**Table 1.** Prior Estimates of the Global or Basin Scale CaCO<sub>3</sub>:Organic Carbon Export Ratio and the Use of These in Models

| Source  | Ratio                              |
|---|------------------------------------|
| <i>Based on Analysis of Observations</i>  |                                    |
| <i>Li et al.</i> [1969]   | 0.25 (0.21 Atlantic, 0.27 Pacific) |
| <i>Broecker</i> [1971]  | 0.11 Atlantic 0.33 Pacific         |
| <i>Broecker and Peng</i> [1982]   | 0.25                               |
| <i>Milliman and Troy</i> [1999]   | 0.05–0.08                          |
| CaCO <sub>3</sub> prod. = 0.60 to<br>0.86 Pg C/yr and <i>Laws et al.</i> [2000] |                                    |
| Org C prod. = 11.1 Pg C/yr  |                                    |
| <i>Lee</i> [2001]   | 0.10–0.12                          |
| <i>Data Analysis with Ocean Biogeochemical Models</i>                           |                                    |
| <i>Yamanaka and Tajika</i> [1996]   | 0.08                               |
| <i>Murnane et al.</i> [1999]  | 0.16                               |
| <i>Used in Ocean Biogeochemical Models</i>                                      |                                    |
| <i>Bacastow and Maier-Reimer</i> [1990]   | 0.15                               |
| <i>Maier-Reimer</i> [1993] <sup>a</sup>   | 0.22                               |
| <i>Archer et al.</i> [2000]   | 0.20                               |
| <i>Aumont</i> [1998] <sup>a</sup>   | 0.25                               |
| <i>Used in OCMIP II Models<sup>b</sup></i>                                      |                                    |
|   | 0.05                               |

<sup>a</sup> *Maier-Reimer* [1993] and *Aumont* [1998] export ratio estimates shown here are obtained from *Sarmiento et al.* [2000].

<sup>b</sup> Ocean Carbon Model Intercomparison Program (OCMIP-II) protocols developed by R. G. Najjar, and J. C. Orr (Design of OCMIP-2 simulations of chlorofluorocarbons, the solubility pump and common biogeochemistry, 1998; available from the World Wide Web at <http://www.ipsl.jussieu.fr/OCMIP/>) were based on the *Yamanaka and Tajika* [1996] ratio of 0.08. However, R. G. Najjar, and J. C. Orr neglected to take into account that the *Yamanaka and Tajika* [1996] study used a particle only model, whereas the OCMIP-II model includes dissolved organic matter. The OCMIP-II model thus erroneously specifies an effective uptake ratio of 0.02, which translates into an export ratio of about 0.05 when surface remineralization of dissolved organic matter is taken into account.

studies estimate the remineralization ratio, i.e., the ratio of CaCO<sub>3</sub> dissolution to organic matter oxidation, not the export ratio. The export ratio and remineralization ratio will equal each other only if there is no loss of organic matter and CaCO<sub>3</sub> from the system, such as to sediments. However, there are additional more significant misinterpretations, as we show in the following. *Li et al.* [1969] used the difference between dissolved inorganic carbon (DIC) and alkalinity (Alk) observations at the surface of the ocean and below 1000 m to claim that about 80% of the excess CO<sub>2</sub> in the deep ocean is derived from the oxidation of organic debris and that the remainder is due to dissolution of CaCO<sub>3</sub>. This gives a CaCO<sub>3</sub> to organic carbon remineralization ratio of  $0.20/0.80 = 0.25$ , ranging from 0.21 in the Atlantic to 0.27 in the Pacific. *Broecker* [1971] used the same data set to obtain estimates of CaCO<sub>3</sub> to total carbon from which one can estimate a CaCO<sub>3</sub> to organic carbon remineralization ratio of 0.11 and 0.33, in the Atlantic and Pacific, respectively, using a different choice of surface concentrations and assuming that roughly half the deep Pacific water comes from the deep Atlantic. Neither *Li et al.* [1969] nor *Broecker* [1971] corrected for the influence of nitrate on the alkalinity. Using the data of *Li et al.* [1969] to make this correction increases their remineralization ratio estimates to 0.24 in the Atlantic and 0.31 in the Pacific. A more appropriate overall remineralization ratio for *Li et al.* [1969] would thus have been

closer to 0.28 rather than to 0.25, with a further increase if they had included the effect of pre-formed concentrations as suggested by the *Broecker* [1971] study.

[5] However, as *Yamanaka and Tajika* [1996] point out, the analysis of *Li et al.* [1969] needs to be further modified if what we actually want to know is the export ratio from the surface of the ocean. Most of the remineralization of organic matter takes place within the thermocline, whereas dissolution of CaCO<sub>3</sub> occurs at greater depth. The remineralization ratio estimated from properties below 1000 m will thus tend to be much higher than the export ratio at the base of the euphotic zone. *Yamanaka and Tajika* [1996] use an ad hoc analysis of the effect of shallow remineralization to suggest that the original *Li et al.* [1969] ratio of 0.25 should be modified to 0.06, plus a correction for sedimentation of CaCO<sub>3</sub> to give a total export ratio of 0.08. (Note that *Yamanaka and Tajika* [1996] also neglected to take the nitrate correction into account, which would increase their export ratio estimate to a value of  $\sim 0.09$ .) They then test this ratio in their ocean biogeochemistry general circulation model and find that it gives good results. However, the use of ocean general circulation models to determine export ratios by fitting or comparison with observations needs to be viewed with caution. For example, *Murnane et al.* [1999] obtain an export ratio of 0.16 in an ocean general circulation model simulation in which they force the horizontally averaged model predicted alkalinity profile to fit the observed horizontal average.

[6] In an attempt to shed further light on the magnitude of the export ratio, we have developed a new method for estimating it based on the ratio of the net supply of Alk and DIC to the surface ocean. Specifically, we calculate the transport divergences of potential alkalinity to salinity normalized nitrate, which we use as a tracer of the DIC supply. If the predominant input of these tracers to the euphotic zone is by vertical advection and mixing, as is generally the case on a large scale, the velocity and apparent vertical diffusivity will cancel when taking the ratio of the inputs, leaving only the ratio of the vertical tracer gradients. It then becomes possible to estimate the net uptake ratio based simply on an analysis of the ratio of the vertical gradients of the tracers. We estimate these gradients using observations obtained by recent global survey data.

## 2. Method

[7] We consider the balance of CaCO<sub>3</sub> and organic carbon in a 100 m thick surface box such as that shown in Figure 1. The box has upwelling  $W$  from below, net horizontal outflow  $U$ , and evaporation minus precipitation ( $E - P$ ) at the air-sea interface. Vertical and horizontal exchanges are represented by the terms  $f$  and  $g$ , respectively. All of the flow rates as well as  $E$ ,  $P$ ,  $f$  and  $g$  are in units of  $\text{m}^3 \text{s}^{-1}$ . The concentration of tracer is in  $\text{mol m}^{-3}$ . The water upwelling into the surface box from below has a concentration  $C_d$ , and the surface concentrations are given as  $C_s$  for the box under consideration and  $C_i$  for inflowing surface water.  $J$  is the net biological uptake and export of tracer from the surface box in  $\text{mol s}^{-1}$ . We will only be considering the balance in the surface box and thus will not concern ourselves with the fate

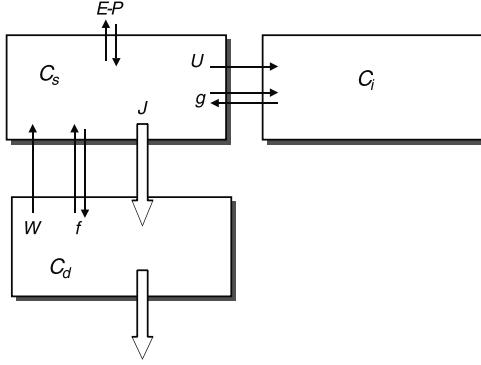


**Figure 1.** Surface ocean biogeochemical-transport box model. See text for a description.

of  $J$  once it leaves the surface. Figure 1 illustrates the situation for water upwelling from below. While the conservation equations are different if the water is downwelling, the final solution for the  $\text{CaCO}_3$  to organic carbon export ratio is identical.

[8] The quantity we are interested in finding is the export ratio,

$$\frac{J_{\text{CaCO}_3}}{J_{\text{organic C}}} \quad (1)$$

Because  $\text{CaCO}_3$  is not measured directly, we relate it to the uptake of alkalinity corrected for the uptake of nitrate,

$$J_{\text{CaCO}_3} = \frac{J_{\text{Alk}} + J_{\text{NO}_3^-}}{2} \quad (2)$$

Furthermore, while the production of organic carbon is directly related to the uptake of dissolved inorganic carbon (DIC), the use of DIC as a tracer for organic carbon cycling is complicated by the fact that DIC can be affected by air-sea gas exchange of  $\text{CO}_2$ . The same problem of having to account for air-sea gas exchange applies to the use of oxygen, which otherwise would be an excellent tracer. We therefore use the uptake of nitrate as a proxy for the net uptake of DIC for production of organic carbon, with an organic C:N stoichiometric molar ratio of 117:16 [Anderson and Sarmiento, 1994], which is a bit higher than the Redfield ratio of 106:16 [Redfield et al., 1963]. We combine (1) and (2) and make use of the C:N ratio of 117:16 in organic matter to obtain

$$\frac{J_{\text{CaCO}_3}}{J_{\text{organic C}}} = \frac{(J_{\text{Alk}} + J_{\text{NO}_3^-})}{2 \cdot (J_{\text{NO}_3^-} \cdot \frac{117}{16})} = \frac{1}{14.6} \frac{(J_{\text{Alk}} + J_{\text{NO}_3^-})}{J_{\text{NO}_3^-}} \quad (3)$$

Note that we ignore the production of organic carbon by nitrogen fixers in the denominator of (3). The global nitrogen fixation rate of about  $110 \text{ Tg N yr}^{-1}$  [Deutsch et al., 2001; Gruber and Sarmiento, 1997] amounts to a carbon uptake of about  $0.69 \text{ Pg C yr}^{-1}$  if one assumes a C:N mole ratio of 117:16 in diazotrophs. This is 6% of the estimated export production of about  $11 \text{ Pg C yr}^{-1}$  [Laws et al., 2000]. The error introduced by neglecting this contribution is thus small relative to other errors in the method, except in areas where fixation is concentrated, such

as the subtropical gyres of the North Atlantic [Gruber and Sarmiento, 1997] and North Pacific [e.g., Karl et al., 1997].

[9] The next step is to use the conservation equations for Alk and nitrate to solve for the  $J$  terms for these two substances in terms of their transport divergence. We then substitute the transport divergence terms into (3). We assume that seasonal and interannual variability are not significant contributors to our calculations, i.e., that we can drop the time derivative, and that the data sets we use can be taken as representative of the annual mean behavior. These assumptions are difficult to justify, given the large seasonal variability and the probable decoupling in time between when calcification occurs and when organic matter formation by noncalcifiers occurs. We have performed several tests of these assumptions using both observations and model simulation results (see section 4), and find that they do not have a significant influence on our conclusions. We believe that this is because the surface to deep property gradients preserve the cumulative history of surface biological uptake until wintertime deep mixing occurs, and most of our data are from periods of time when deep mixing was not occurring. The steady state tracer balance equation for the surface box in Figure 1 is then

$$J = W \cdot C_d + f \cdot (C_d - C_s) + g(C_i - C_s) - U \cdot C_s \quad (4)$$

This can be rearranged to give

$$J = (W + f) \cdot (C_d - C_s) + g(C_i - C_s) + (W - U) \cdot C_s \quad (5)$$

We solve the salinity balance equation

$$0 = W \cdot S_d - U \cdot S_s + f(S_d - S_s) + g(S_i - S_s) \quad (6)$$

for  $U$  and substitute this into (5) to obtain

$$J = (W + f) \cdot S_d \cdot \left( \frac{C_d - C_s}{S_d - S_s} \right) + g \cdot S_i \cdot \left( \frac{C_i - C_s}{S_i - S_s} \right) \quad (7)$$

We now substitute (7) into (3), divide by  $S_d$  and the transport terms  $(W + f)$ , and make use of the following definitions for potential alkalinity following Brewer et al. [1975] and salinity normalized nitrate

$$\begin{aligned} P_{\text{Alk}} &= (\text{Alk} + \text{NO}_3^-) \cdot \frac{35}{S} \\ n\text{NO}_3^- &= \text{NO}_3^- \cdot \frac{35}{S} \end{aligned} \quad (8)$$

respectively, in order to obtain

$$\frac{J_{\text{CaCO}_3}}{J_{\text{organic C}}} = \frac{1}{14.6} \frac{\left[ (P_{\text{Alk}_d} - P_{\text{Alk}_s}) + \frac{g}{W+f} \cdot \frac{S_i}{S_d} \cdot (P_{\text{Alk}_i} - P_{\text{Alk}_s}) \right]}{\left[ (n\text{NO}_3^-_d - n\text{NO}_3^-_s) + \frac{g}{W+f} \cdot \frac{S_i}{S_d} \cdot (n\text{NO}_3^-_i - n\text{NO}_3^-_s) \right]} \quad (9)$$

In general, we expect that the lateral tracer gradient in the second term of both the numerator and denominator will be smaller than the vertical gradient in the first term. In addition, on the space scales we are considering, the replacement of mixed layer waters with respect to lateral exchange will have a timescale of many years. Replacement by vertical processes generally occurs on timescales of less

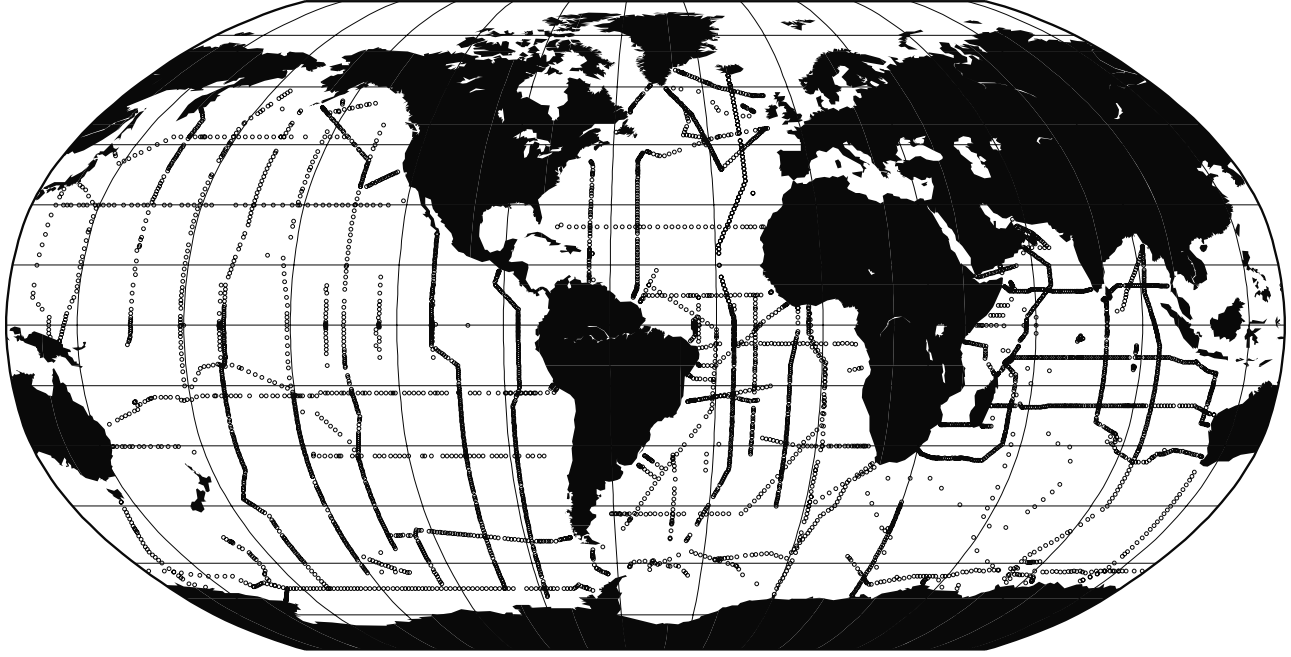


**Figure 2.** Map of stations used in the analysis of the  $\text{CaCO}_3$  to organic carbon export ratio.

than a year such that  $(W+f) \gg g$ . We therefore assume that the second term of both the numerator and denominator can be neglected relative to the first term, giving us the final equation

$$\frac{J_{\text{CaCO}_3}}{J_{\text{organic C}}} = \frac{1}{14.6} \frac{P_{\text{Alk}_d} - P_{\text{Alk}_s}}{n\text{NO}_{3d}^- - n\text{NO}_{3s}^-}. \quad (10)$$

This equation shows that we can estimate the ratio of  $\text{CaCO}_3$  to organic carbon export from the vertical gradients of potential alkalinity and salinity normalized nitrate without needing to specify the actual magnitude of the transport terms.

### 3. Data and Analysis

[10] The data set used for our calculations is taken from the stations shown in Figure 2. For the Indian Ocean, data was restricted to WOCE (World Ocean Circulation Experiment) stations plus measurements from the French INDIGO expedition [cf. *Sabine et al.*, 1999]. For the Pacific Ocean, data was limited to WOCE stations plus a small amount of additional data from recent NOAA OACES cruises [cf. *Lamb et al.*, 2002; *Sabine et al.*, 2002]. On a few Pacific cruises where alkalinity was not measured, but at least 2 of the carbon system parameters were measured (total inorganic carbon, pH,  $\text{pCO}_2$ ), alkalinity values were calculated using *Mehrbach et al.* [1973] data as refit by *Dickson and Millero* [1987]. A summary of the Atlantic data set is shown in Table 2. There are no data from the Arctic Ocean or Mediterranean seas.

[11] We calculate the  $\text{CaCO}_3$  to organic carbon export flux ratio at a depth of 100 m. The surface concentration at each station is taken as the mean over the top 100 m, and the deep concentration as the mean over 100 to 200 m, which

we symbolize by the expressions  $\langle \rangle_{0-100\text{ m}}$  and  $\langle \rangle_{100-200\text{ m}}$ , respectively. The ratio is calculated over  $N$  stations covering a large region, as described below.

$$\left( \frac{J_{\text{CaCO}_3}}{J_{\text{organic}}} \right)_{100\text{ m}} = \frac{1}{14.6} \cdot \frac{\left[ \sum_{i=1}^N (\langle P_{\text{Alk}} \rangle_{100-200\text{ m}} - \langle P_{\text{Alk}} \rangle_{0-100\text{ m}})_i \right]}{\left[ \sum_{i=1}^N (\langle n\text{NO}_3^- \rangle_{100-200\text{ m}} - \langle n\text{NO}_3^- \rangle_{0-100\text{ m}})_i \right]}. \quad (11)$$

Our choice of 100 m as the depth at which we define the export flux ratio follows the common practice of many biogeochemical analyses such as the particulate flux studies of *Martin et al.* [1987] and *Bishop* [1989]. Our decision to define the deep box as having a depth range of 100 to 200 m was made after considering several alternatives, including calculating the slope at 100 m from a curve fit to upper ocean observations. One can readily show from the tracer balance equation that the right hand side of (9) can also be found by calculating the ratio of the vertical slope of  $P_{\text{Alk}}$  to that of normalized nitrate. A curve fit approach would have been our preference, but the poor signal-to-noise ratio for potential alkalinity, and the sparseness of measurements in the upper ocean, led to high uncertainties in slopes estimated by this method.

[12] The use of box averages to calculate the gradient requires that a thickness be specified for the deep box. Too thin a box (e.g., a depth range of 100 to 150 m) leads to increased uncertainty because of the sparseness of data and the small magnitude of the vertical gradient relative to the measurement precision. Both potential alkalinity and nitrate increase more or less exponentially with depth below the mixed layer. One can thus improve the precision of the gradient estimate, as well as include more measurements, by increasing the depth range. However, because of the shal-

**Table 2.** Atlantic Ocean Cruises Used in This Study<sup>a</sup>

| Line      | Cruise          | Chief Scientist                | Carbon System Investigator          | References Where Available  |
|-----------|-----------------|--------------------------------|-------------------------------------|---|
| Leg I     | AJAX            | J. Reid                        | T. Takahashi                        | <i>Oceanographic Data Facility</i> [1985],<br><i>Chipman and Takahashi</i> [1986] |
| Leg II    | AJAX            | W. Nowlin                      | T. Takahashi                        | <i>Oceanographic Data Facility</i> [1985],<br><i>Chipman and Takahashi</i> [1986] |
| Leg 1     | SAVE            | T. Takahashi, P. Rhines        | T. Takahashi                        | <i>Oceanographic Data Facility</i> [1992b]  |
| Leg 2     | SAVE            | W. Smethie, S. Jacobs          | T. Takahashi                        | <i>Oceanographic Data Facility</i> [1992b]  |
| Leg 3     | SAVE            | W. Jenkins, D. Olson           | T. Takahashi                        | <i>Oceanographic Data Facility</i> [1992b]  |
| Leg 4     | SAVE            | R. Key, A. Piola               | T. Takahashi                        | <i>Oceanographic Data Facility</i> [1992c]  |
| Leg 5     | SAVE            | W. Smethie, M. McCartney       | T. Takahashi                        | <i>Oceanographic Data Facility</i> [1992c]  |
| Leg 4     | HYDROS          | L. Talley, M. Tsuchiya, J. Orr | T. Takahashi                        | <i>Oceanographic Data Facility</i> [1992a]  |
| Leg 1,2   | OACES91_1/2     | D. Wilson                      | R. Wanninkhof, F. Millero           |   |
| Leg 1,2,3 | OACES93_1/2/3   | E. Johns, R. Wanninkhof        | R. Wanninkhof, F. Millero, R. Feely |   |
| A1E       | 06MT18/1        | J. Meincke                     | D. Wallace, L. Mintrop              | <i>Johnson et al.</i> [1996]  |
| A1W       | 18HU95011/1     | J. Lazier                      | R. Gershey                          |   |
| A2        | 06MT039_3       | P. Koltermann                  | D. Wallace                          |   |
| A5        | 29HE06_1        | G. Parrilla                    | F. Millero                          | <i>Millero et al.</i> [2000]  |
| A6        | 35A3CITHER1_2   | C. Oudot                       | C. Oudot                            |   |
| A7        | 35A3CITHER1_1   | A. Morliere                    | C. Oudot                            |   |
| A14       | 35A3CITHER3_1   | M. Arhan                       | M. Gonzalez                         |   |
| A15       | 316N142/3       | W. Smethie, G. Weatherly       | C. Goyet                            |   |
| A17       | 3230CITHER2_1/2 | L. Memery                      | A. Rios                             |   |
| A20       | 316N151-3       | R. Pickart                     | F. Millero, C. Sabine               |   |
| A21       | 06MT11_5        | W. Roether                     | T. Takahashi                        | <i>Chipman et al.</i> [1994]  |
| A22       | 316N151_4       | T. Joyce                       | F. Millero, C. Sabine               |   |
| A24       | 316N151_2       | L. Talley                      | F. Millero                          |   |

<sup>a</sup>Data from the two Ocean Atmosphere Carbon Exchange Study (OACES) cruises can be obtained from the World Wide Web server at [http://www.aoml.noaa.gov/ocd/oaces/bottle\\_data.html](http://www.aoml.noaa.gov/ocd/oaces/bottle_data.html). All lines beginning with the letter A are WOCE (World Ocean Circulation Experiment) Hydrographic Office) cruises. The nutrient data and Chief Scientist's cruise reports for WOCE lines are available from the WOCE Hydrographic Office (University of California at San Diego, Scripps Institution of Oceanography, La Jolla, California; World Wide Web server at <http://whpo.ucsd.edu>). The carbon data for the AJAX and WOCE lines are available from the Carbon Dioxide Information Analysis Center, Environmental Sciences Division, Oak Ridge National Laboratory, U. S. Department of Energy (World Wide Web server at <http://cdiac.esd.ornl.gov>). Note, that the Indian Ocean and Pacific Ocean data that we used are described in detail by *Sabine et al.* [1999], *Lamb et al.* [2002], and *Sabine et al.* [2002].

lower remineralization of nitrate relative to dissolution of  $\text{CaCO}_3$ , one runs the risk that calculating the gradient over a wider depth range will bias the  $P_{Alk}$  gradient toward higher values relative to the vertical gradient of nitrate. When testing the method in an ocean general circulation model (OGCM; as described later in this paper) we found that increasing the thickness of the lower layer to 150 m resulted in an increase in the estimated export ratio of 0.01–0.02, and increasing it to 200 m resulted in a further increase of 0.01–0.013. We found that a thickness of 100 m was a reasonable compromise that gave acceptable results in all the tests we performed, as discussed below.

[13] The export ratios are estimated over 14 regions comprising the tropics ( $15^\circ\text{S}$  to  $15^\circ\text{N}$ ) and subtropical and subpolar gyres (broken at  $45^\circ$ ) of each hemisphere of the Atlantic, Indian, and Pacific Ocean basins. An alternative would be to do the calculation at each station individually. However, it is less likely that our assumptions would be satisfied locally than on a large scale. Furthermore, the error in the export ratios becomes extremely large because of the poor signal-to-noise ratio of  $P_{Alk}$  and the difficulty of estimating a meaningful ratio where the vertical normalized nitrate gradient is close to zero. These problems are illustrated in Figure 3, which shows plots of the  $P_{Alk}$  gradient versus the normalized nitrate gradient for all the stations in each of the above regions. The large scatter in the data is due almost exclusively to the low signal relative to the measurement precision of alkalinity measurements. Note also that there are a large number of stations with vertical

nitrate gradients near zero. Such stations would tend to give extremely variable ratios with values approaching  $\pm\infty$ , which have no biogeochemical meaning. After testing a wide range of methods using techniques described in the following section, we found that the best way to estimate the overall ratio of gradients was to take the ratio of the sums, as in (11). One alternative that we tested was a simple least squares linear regression using the individual data shown in Figure 3. This method gives preferential weight to the data that deviate the most from the regression line, and gives export ratios that are biased high relative to the actual ratio.

[14] We use the bootstrap method to estimate the non-parametric standard deviation of the mean. We construct 10,000 trial data sets from the original data set by random selection with replacement (i.e., repeatedly randomly selecting from the same set of observations). The “best” estimate of the gradient is the median of all the individual estimates, and the 95% confidence limits come directly from the 2.5% and 97.5% tails of the resulting distribution. The bootstrap method gives a more robust estimate of the uncertainty, particularly in cases where the distribution of estimates is non-Gaussian. If the distribution of estimates is Gaussian, then the two methods are equivalent. The slope and confidence limits estimated in this fashion are shown in Figures 3 and 4. One can see from the confidence limit estimates that the slope is very tightly constrained by the measurements despite the large scatter in them. However, it needs to be emphasized that the 95% confidence limits provide only

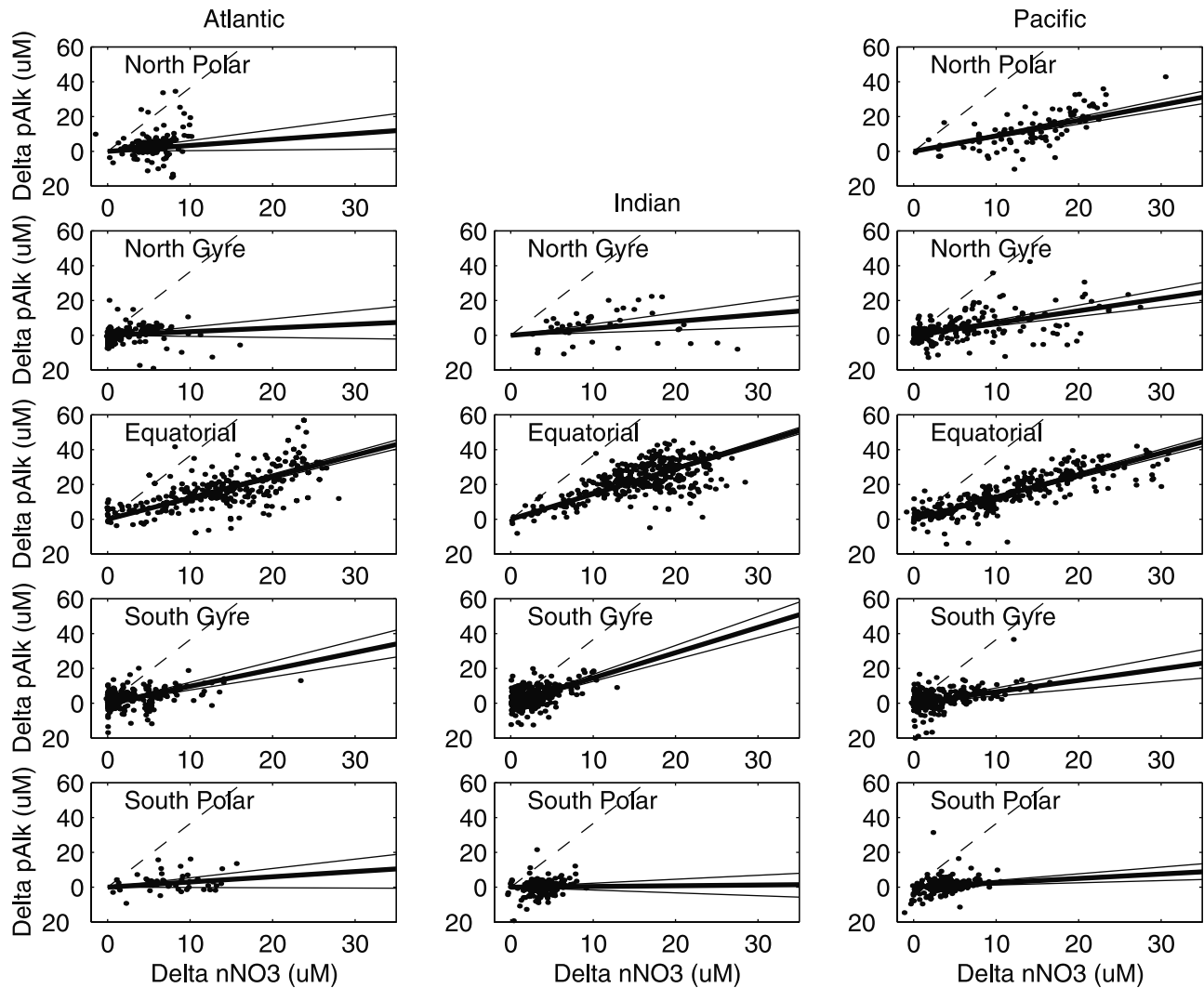


**Figure 3.** Plot of vertical  $P_{Alk}$  versus  $nNO_3$  gradients for each station. The dashed line has a slope of 0.25 following the estimated export ratios of *Li et al.* [1969]. The solid lines are the median estimate of the slope from the data with 95% confidence limits.

a measure of how the average gradient estimate would vary if one were to repeatedly make the same number of measurements and obtain an independent estimate of the average gradient each time. They are not a measure of absolute error; that is, the actual answer might lie outside the bounds of the bootstrap error if there are systematic sources of bias or natural variability in the ratio.

#### 4. Results and Discussion

[15] Table 3 shows our estimated  $CaCO_3$  to organic carbon export ratios and Figure 4 shows them plotted versus latitude. The main result of this analysis is that the export ratio is everywhere  $<0.10$ , with an area weighted mean of  $0.056 \pm 0.004$  (the uncertainty is calculated by least squares propagation of the bootstrap errors shown in Table 3). This is consistent with the study of *Yamanaka and Tajika* [1996] in showing that the much higher ratios obtained from analyses of surface versus deep water data by *Li et al.*

[1969] and *Broecker* [1971] are not appropriate indicators of surface ocean export ratios.

[16] We ran two tests in order to examine potential sources of systematic error in our estimate. The first was to determine whether one could use our method and the same data set to obtain estimates of the N:P ratio that would be comparable to the expected N:P Redfield ratio of 16 [*Redfield et al.*, 1963]. The N:P export ratios in Figure 5 show excellent agreement with the Redfield ratio in the Atlantic Ocean, with a tendency for the Pacific and Indian Oceans to have somewhat lower values. These results will be discussed in more detail in a separate publication. We would make two points at this time, the first being that lower than Redfieldian N:P export ratios may be reasonable in light of suggestions that organic phosphorus is recycled more efficiently than organic nitrogen [e.g., *Martin et al.*, 1987] and the finding that ratios estimated from observations below  $\sim 400$  m are closer to the Redfield value of 16 [cf. *Anderson and Sarmiento*, 1994; *Shaffer et al.*, 1999].

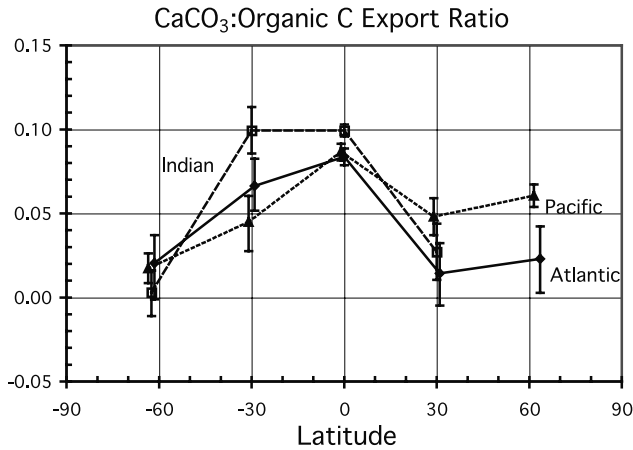


**Figure 4.**  $\text{CaCO}_3$  to organic carbon export ratio estimated from observations. Each symbol represents the horizontal average over a region that goes from the Antarctic to  $45^\circ\text{S}$ , from  $45^\circ\text{S}$  to  $15^\circ\text{S}$ , and from  $15^\circ\text{S}$  to  $15^\circ\text{N}$ , with corresponding areas in the northern hemisphere between  $15^\circ\text{N}$  and  $45^\circ\text{N}$ , and poleward of  $45^\circ\text{N}$ .

The second point is that we are encouraged that the lack of seasonal resolution in the measurements does not appear to have a major impact on the N:P ratio estimate. There is some tendency toward a systematic behavior of the errors in the N:P estimate. The N:P ratio estimate may be somewhat low in the Pacific and Indian Oceans. However, the lowest estimate is only 30% below the canonical ratio of 16, and as we suggest, one can make a case that this may be realistic. This result is perhaps less surprising than it might seem at first glance, since one might expect the supply ratio to be

**Table 3.** Estimates of  $\text{CaCO}_3$ :Organic Carbon Export Ratio From This Study

| Region  | Number of Stations | Median Ratio <sup>a</sup> |
|---|--------------------|---------------------------|
| <i>Atlantic Ocean</i>                                     |                    |                           |
| Subpolar gyre ( $>45^\circ\text{N}$ )                     | 170                | $0.023 \pm 0.020$         |
| Subtropical gyre ( $15^\circ\text{N}-45^\circ\text{N}$ )  | 185                | $0.014 \pm 0.019$         |
| Equatorial region ( $15^\circ\text{S}-15^\circ\text{N}$ ) | 304                | $0.084 \pm 0.005$         |
| Subtropical gyre ( $45^\circ\text{S}-15^\circ\text{S}$ )  | 204                | $0.066 \pm 0.016$         |
| Southern Ocean subpolar gyre ( $<45^\circ\text{S}$ )      | 50                 | $0.020 \pm 0.022$         |
| <i>Indian Ocean</i>                                       |                    |                           |
| Subtropical gyre ( $15^\circ\text{N}-45^\circ\text{N}$ )  | 43                 | $0.027 \pm 0.017$         |
| Equatorial region ( $15^\circ\text{S}-15^\circ\text{N}$ ) | 352                | $0.099 \pm 0.004$         |
| Subtropical gyre ( $45^\circ\text{S}-15^\circ\text{S}$ )  | 305                | $0.099 \pm 0.014$         |
| Southern Ocean subpolar gyre ( $<45^\circ\text{S}$ )      | 155                | $0.003 \pm 0.013$         |
| <i>Pacific Ocean</i>                                      |                    |                           |
| Subpolar gyre ( $>45^\circ\text{N}$ )                     | 97                 | $0.061 \pm 0.007$         |
| Subtropical gyre ( $15^\circ\text{N}-45^\circ\text{N}$ )  | 195                | $0.048 \pm 0.011$         |
| Equatorial region ( $15^\circ\text{S}-15^\circ\text{N}$ ) | 302                | $0.087 \pm 0.005$         |
| Subtropical gyre ( $45^\circ\text{S}-15^\circ\text{S}$ )  | 282                | $0.045 \pm 0.017$         |
| Southern Ocean subpolar gyre ( $<45^\circ\text{S}$ )      | 236                | $0.017 \pm 0.009$         |

<sup>a</sup> The uncertainty that is shown is the larger of the 2.5% or 97.5% tails of the bootstrap distribution. In most cases, the two are equal to each other (see Figure 4).

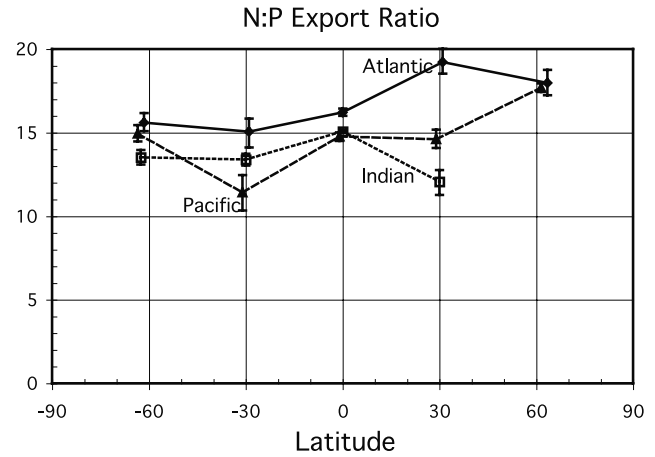


**Figure 5.** N:P export ratio estimated from observations.

preserved in the water property distributions as long as it is not destroyed by deep wintertime mixing. Only a few of the observations were made during local winter conditions when such mixing would cause problems.

[17] The second test we ran was to estimate the vertical export gradient using distributions generated by an OGCM simulation where we know the underlying fluxes and can determine their actual ratios exactly. The OGCM we used is the KVHISOUTH + AILOW model described by *Gnanadesikan et al.* [2002]. The model “data” were monthly ratios that were sub-sampled numerous times with the same sampling frequency as the “real” observations, though not exactly at the same locations. Figure 6 shows the estimated and actual export ratios from the model. The 95% error bounds shown for the estimated export ratio are from the bootstrap calculation. We added randomly varying “analytical error” to the model “data” in order to make the error limits more directly comparable to the error limits obtained from analysis of the observations. The assumed analytical error was  $4 \text{ eq}^{-1}$  for alkalinity and  $0.45 \mu\text{mol L}^{-1}$  for nitrate (1% of the maximum observed nitrate of  $45 \mu\text{mol L}^{-1}$ ), with 2 data points in each layer (a conservative estimate, since the number of data points averaged 2 to 4). The agreement between the estimated and actual export ratios is mostly quite good, but there are regions where the actual ratios are not within the error bars of the estimated ratio, which indicates that there are biases in the estimated ratio. In particular, there is a tendency for the estimated export ratio to exceed the actual export ratio in the subpolar gyres of both the northern hemisphere and Southern Ocean, and to underestimate the ratio in some of the subtropical gyres. The maximum bias in the export ratio estimate is approximately  $\pm 0.03$ .

[18] The exact cause of differences between the estimated and true export ratios is difficult to diagnose, since it requires recalculating the OGCM transport terms in the same form as the box model, which we have not done. However, a likely explanation is a violation of our assumptions that vertical processes dominate over lateral ones (i.e.,  $(W + f) \gg g$ ) and that vertical gradients in alkalinity and nitrate are much larger than lateral gradients. The concentrations of both nitrate and alkalinity are high in the Southern

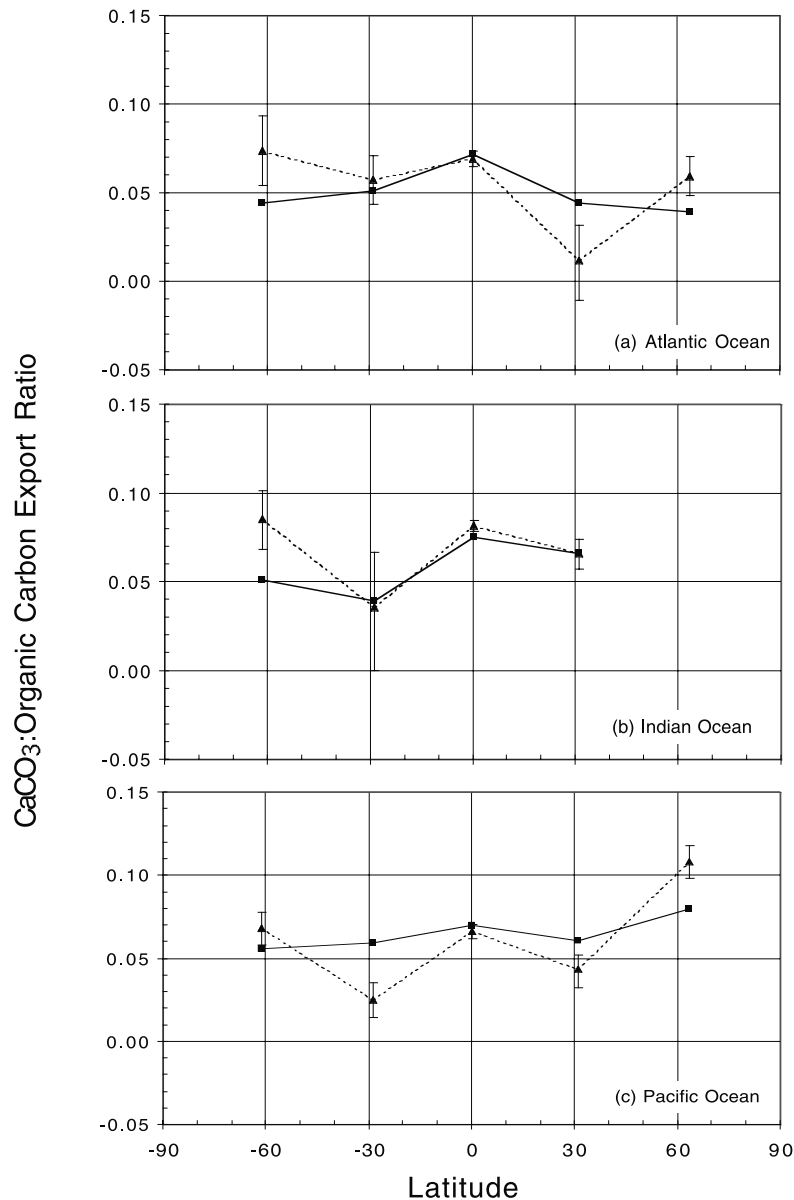


**Figure 6.** CaCO<sub>3</sub> to organic carbon export ratio from the ocean general circulation model described by *Gnanadesikan et al.* [2002]. The solid line and squares are the actual export ratios estimated over the same latitude bands as in Figure 4. The dashed lines and triangles are estimated ratios found as described in the text.

Ocean and subpolar gyres of the northern hemisphere. However, nitrate tends to be stripped out within the subpolar gyres (defined here as poleward of 45°), whereas the high alkalinity gradient persists more strongly into the boundary of the subpolar gyre regions that we have defined at 45°N and S. Thus, the horizontal gradient of alkalinity may be somewhat large relative to its vertical gradient, whereas that of nitrate may be smaller relative to its vertical gradient. These are both negative corrections that would tend to reduce the export ratio. Consideration of the vertical gradient alone without these corrections may be what gives too high an export ratio in most of the subpolar gyre regions.

[19] The tendency toward a low ratio in the subtropics very likely results from a similar problem to that in the

subpolar gyre only the situation is more complicated to analyze because the sign of  $W$  is negative (downwelling) and there is exchange with the equatorial band. Despite  $W$  being negative, the transport ratio  $g/(W + f)$  should generally be positive, because  $f > |W|$  due to the large amount of vertical exchange  $f$  resulting from convective overturning as well as mixing. This being the case, exchange with the subpolar gyre will tend to increase the numerator of (9) more than the denominator. Leaving this correction out, as we do, will give an underestimate of the export ratio, as observed. On the other hand, the equatorial band has low alkalinity and high nitrate, such that lateral input from this band will tend to reduce the numerator of (9) and increase its denominator. Leaving this correction out may thus



**Table 4.** Local Estimates of the CaCO<sub>3</sub>:Organic Carbon Export Ratio

| Source                                   | Method   | Location                             | Ratio                  |
|--|--|--------------------------------------|------------------------|
| <i>North Atlantic</i>                    |  |                                      |                        |
| <i>Takahashi et al.</i> [1990]           | surface concentration gradient                                   | 47°N, 20°W                           | 0.12 ± 0.02            |
| <i>Kortzinger et al.</i> [2001]          | surface concentration gradient                                   | ~30°–60°N, 20°W                      | undetectable           |
| <i>North and Equatorial Pacific</i>      |  |                                      |                        |
| <i>Tsunogai and Noriki</i> [1991]        | shallow sediment trap (125 m)                                    | 41°N, 142°E                          | 0.01                   |
| <i>Rodier and Le Borgne</i> [1997]       | shallow sediment trap (105 m)                                    | 0°N, 167°E                           | 0.21                   |
|  | shallow sediment traps   | 0°N, 150°W                           | 0.11                   |
| <i>Wanninkhof et al.</i> [1995]          | surface concentration gradient<br>in Southern Equatorial Current | 3°S–0°S, 110°W–140°W                 | 0.13 spring, 0.22 fall |
| <i>Southern Ocean</i>                    |  |                                      |                        |
| <i>Bates et al.</i> [1998]               | surface concentration gradient                                   | 76.5°S, 160°E–170°W Ross Sea Polynya | undetectable           |
| <i>Rubin et al.</i> [1998]               | surface seasonal concentration change                            | 72°S–67°S, 110°W–170°W               | undetectable           |
| <i>Sweeney et al.</i> [2000]             | surface concentration variability                                | Ross Sea                             | ≤0.05                  |
| <i>McNeil et al.</i> [2001] <sup>a</sup> | surface seasonal concentration change                            | 50°S–45°S, 140°E                     | undetectable           |

<sup>a</sup>B.I. McNeil, B. Tilbrook, and R.J. Matear, Carbon export in the sub-Antarctic zone, South Of Australia based on seasonal changes in DIC and DIC-C13, submitted to *Deep Sea Research, Part I*, 2001.

partially counteract the effect of leaving out the subpolar gyre lateral exchange term.

[20] Overall, our tests indicate that our method can determine the export ratio to within about ±0.03. The estimated ratios tend to be high in higher latitudes and low in the subtropics. These systematic features need to be kept in mind as we consider the spatial distribution of our estimates.

[21] The regional distribution of our export ratio estimates shows a high in the equatorial region, with a tendency to decrease with increasing latitude (Figure 4 and Table 3). A region where this result is somewhat at odds with expectations from previous observations is the North Atlantic subpolar gyre, where we obtain an export ratio of only  $0.023 \pm 0.020$ . This is an area that satellite and other observations indicate is exceptionally rich in coccolithophore blooms (see especially *Brown and Yoder* [1994] and *Iglesias-Rodríguez et al.* [2002], as well as *Holligan et al.* [1993], *Fernández et al.* [1993], and *Ziveri et al.* [2000]). The systematic bias that we found in testing our method with model simulation results would suggest that we should, if anything, overestimate the ratio in this region. There are times and places where the impact of CaCO<sub>3</sub> formation can clearly be seen in the potential alkalinity distribution [e.g., *Takahashi et al.*, 1990] (see Table 4). The local impact of a major bloom can be particularly dramatic [*Robertson et al.*, 1994]. The sediment and deep sediment trap records [e.g., *Archer*, 1996; *Milliman*, 1993] show the North Atlantic to be, if anything, an area of high carbonate production. However, there are also times when this region does not exhibit a discernable drawdown of potential alkalinity [*Kortzinger et al.*, 2001] (see Table 4). The observations that we have in this region are too limited to determine whether our results might be biased due to lack of sufficient spatial and temporal resolution.

[22] Other regions of the world where the vertical potential alkalinity gradient and resulting export ratios are small include the subtropical gyre of the North Atlantic, and all three regions of the Southern Ocean (see Figure 3). However, contrary to our results in the North Polar Atlantic, the low ratios in these regions are more in line with expectation.

For example, measurements of salinity normalized alkalinity at the Bermuda Atlantic Time Series station in the Sargasso Sea indicate that a detectable drawdown of alkalinity is extremely rare. *Bates et al.* [1996] and *Bates* [2001] observe only two significant drawdown episodes between 1991 and 1998, in February 1992 and January 1998. Observations from the Southern Ocean summarized in Table 4 also show undetectable drawdown ratios.

[23] The areas where we obtain high export ratios also tend to be supported by independent observations in the few places where these are available. The North and equatorial Pacific are particularly well documented, with drawdown ratios (see Table 4) and observations of calcification versus photosynthesis [*Fabry*, 1989; *Balch and Kilpatrick*, 1996] showing variable but generally high ratios consistent with those that we obtain in these regions. The same is true of the Indian Ocean, where the Arabian Sea observations of *Balch et al.* [2000] gave calcification rates that were 1–5% of estimated primary production.

[24] Sediment traps provide the only direct means of estimating the CaCO<sub>3</sub> to particulate organic carbon export ratio, but are prone to strong collection biases due to hydrodynamics, zooplankton interference, and sediment resuspension (coastal studies only). In the JGOFS equatorial Pacific program, both conical (Indented Rotating Sphere, or IRS [*Hernes et al.*, 2001]) and cylindrical (particle interceptor trap, or PIT [*Murray et al.*, 1996]) sediment traps were deployed. While similar CaCO<sub>3</sub> fluxes were obtained from IRS traps ( $1.8 \pm 1.1 \text{ mmol m}^{-2} \text{ d}^{-1}$  [*Hernes et al.*, 2001]) and PITs ( $2.0 \pm 3.2 \text{ mmol m}^{-2} \text{ d}^{-1}$ ; J. Murray and J. Newton, personal communication, 2002), organic carbon fluxes were  $7 \pm 4$  times higher in PITs than in IRS traps, leading to drastic differences in the inferred rain ratio, from CaCO<sub>3</sub>:Corg values in PITs of  $0.13 \pm 0.13$  to values in IRS traps of  $0.7 \pm 0.5$ . Comparisons between measured and modeled <sup>234</sup>Th suggested undercollection of <sup>234</sup>Th and organic carbon by IRS traps (factor of  $5 \pm 9$  [*Hernes et al.*, 2001]) and overcollection by PITs (factor of  $2 \pm 5$  [*Murray et al.*, 1996]). Since these two traps collected similar amounts of CaCO<sub>3</sub>, this demonstrates extensive differentiation of particles between traps. Assuming that

both traps were accurate collectors of  $\text{CaCO}_3$ , and calibrating the organic carbon flux with  $^{234}\text{Th}$  gives a resultant  $\text{CaCO}_3$ :organic carbon export ratio of 0.16 to 0.27. These estimates are extremely uncertain, however, as they are based on bold assumptions about differential particle collection efficiency and  $^{234}\text{Th}$  particle associations.

[25] The sparse network of direct observations of calcification described above makes it difficult to verify the pattern of export ratios that we obtain. The only global scale observations that might be used for this purpose are the satellite based estimates of coccolithophore blooms by *Brown and Yoder* [1994] and *Iglesias-Rodríguez et al.* [2002]. These estimates clearly indicate that coccolithophore blooms are found primarily in high latitudes of both hemispheres, with essentially no blooms in low latitudes. Anecdotal evidence and a few published measurements suggest that coccolithophores comprise perhaps two thirds of open ocean calcification [*Fabry*, 1989; B. Balch, personal communication, 2002]. How much of this is contributed by the blooms that are observed in the satellite data? *Brown and Yoder* [1994] estimate that these blooms can account for a conservative lower limit of 0.3% of the total calcification estimates summarized by *Sundquist* [1985], and that this might be increased by an order of magnitude if they modified some of the assumptions in their model. They conclude that populations not detected by the satellite observations must produce most of the coccoliths found in sediments. In their discussion of the response of the oceans to global warming, *Iglesias-Rodríguez et al.* [2002] assume that the behavior of bloom coccolithophores can be used to characterize the behavior of all coccolithophores, with coccolithophores accounting for 80% of the calcification. Our observations are consistent with the more conservative interpretation of *Brown and Yoder* [1994].

[26] Given the high level of uncertainty in our estimates of the magnitude of the export ratio, we would like to make some comments on the types of measurements that could help to further constrain the export ratio. One way of estimating the export ratio is by measuring the  $\text{CaCO}_3$  and particulate organic carbon caught in sediment traps. Estimates made in this way range widely from less than 0.1 to values as high as 1.0. (see Table 3 and discussion above). However, the methodological problems with sediment traps, which have been explored widely in the literature [e.g., *Buesseler*, 1991; *Honjo*, 1996], continue to be an issue, as illustrated by the equatorial Pacific measurements discussed above.

[27] A second way to estimate the stoichiometric ratios of export from the surface ocean is by using the property gradients along isopycnal surfaces to estimate the remineralization ratio [e.g., *Minster and Boulahdid*, 1987]. This assumes that the material being remineralized on a given isopycnal surface has the same ratio as the material being exported from the surface. *Anderson and Sarmiento* [1994] have used this method to estimate the remineralization ratio of organic carbon, nitrate, and phosphate, as well as  $\text{CaCO}_3$ . However, it is clear from their analysis, as well as numerous other studies [e.g., *Tsunogai and Noriki*, 1991] that organic carbon is remineralized at much shallower depths in general than those where dissolution of  $\text{CaCO}_3$  occurs. Further-

more, *Anderson and Sarmiento* [1994] were not able to apply their method of analysis above about 400 m. This leaves out the part of the water column where most of the remineralization of organic matter occurs [e.g., *Martin et al.*, 1987], but only a small fraction of the  $\text{CaCO}_3$  dissolution occurs [*Milliman and Troy*, 1999].

[28] A third approach to determining the export ratio is to estimate the net biological uptake of the tracers from the tracer transport divergence. In a steady state, the net input of tracer by transport must equal the export of biogenic material. Thus, for example, the biological uptake of tracer at the surface can be estimated by calculating the net input of tracer by advection and diffusion [e.g., *Ganachaud*, 1999; *Murnane et al.*, 1999; *Rintoul and Wunsch* [1991]. A major difficulty with this approach is that it requires estimating the advection and diffusivity, which is difficult to do with sufficiently high precision.

[29] We thus conclude that the best way of estimating the export ratio is through direct observations of the reduction in surface DIC, Alk, and nitrate over a period of time. The estimate of *Lee* [2001] reported in Table 1 uses a method based on this approach. However, since the actual observations of DIC and Alk are so sparse, he must resort to an ad hoc extrapolation based on empirical algorithms that describe the relationship between DIC and Alk to the more abundant sea surface temperature and nitrate data. His global mean ratio of 0.10 to 0.12 is larger than our global average of  $0.06 \pm 0.03$ . An examination of the regional breakdown of the ratios we calculate from his flux estimates reveals that most of the discrepancy is in the high latitudes of the Atlantic and Southern Ocean. As noted earlier, the model based tests suggest that our method will overestimate the export ratios in these regions, which goes the wrong way toward reconciling them with of *Lee* [2001]. We need more measurements to resolve this issue. Such measurements are difficult to obtain and have only been made at a few locations.

[30] The method we have proposed here works well where the signal is strong and the measurement resolution is high in both space and time. In situ observations of calcification and primary production such as those obtained by *Balch and Kilpatrick* [1996], are potentially very powerful, but without an estimate of the  $f$ -ratio (the ratio of new to primary production) and surface  $\text{CaCO}_3$  dissolution, their utility for determining the export ratio is limited.

[31] If we take our global average export ratio of 0.056, and multiply it by the global organic carbon production estimate of *Laws et al.* [2000], 11 Pg C/yr, we estimate that the  $\text{CaCO}_3$  export amounts to 0.6 Pg C/yr. This is consistent with the estimate of 0.70 Pg C/yr that *Milliman and Troy* [1999] give. *Lee* [2001] estimates twice as much  $\text{CaCO}_3$  export as we do, but, as already noted, his assessment is obtained by an ad hoc extrapolation of sparse alkalinity data using correlations to other data with better seasonal resolution.

[32] We conclude that the global  $\text{CaCO}_3$ :organic carbon export ratio is about  $0.06 \pm 0.03$ . Even taking into consideration the systematic error of  $\sim 0.03$  identified in the tests of our method, our results clearly indicate that the export ratio is unlikely to be anywhere near as large as the value of

0.20 to 0.25 used in some modeling studies [e.g., Archer *et al.*, 2000; Maier-Reimer, 1993; and Aumont, 1998]. Our results suggest that the export ratio is highest in the tropics and decreases toward the poles. We are less confident of the spatial distribution of our results than we are of the global mean and would encourage further exploration of this issue both by measurements as well as by model sensitivity studies.

[33] **Acknowledgments.** This paper was greatly improved by lively interactions with Niki Gruber, Andy Jacobson, Danny Sigman, and Patrick Monfray, as well as perspicacious readings by Robbie Toggweiler and the three reviewers, including David Archer. The Carbon Modeling Consortium carried out the project described in this article with support from NOAA's Office of Global Programs (grant NA96GP0312). Additional support was provided by the Ocean Carbon Sequestration Research Program, Biological and Environmental Research (BER), U. S. Department of Energy (grant DE-GG02-00ER63009); and by the National Science Foundation (grant OCE-0097316).

## References

- Anderson, L. A., and J. L. Sarmiento, Redfield ratios of remineralization determined by nutrient data analysis, *Global Biogeochem. Cycles*, 8(1), 65–80, 1994.
- Archer, D. E., An atlas of the distribution of calcium carbonate in sediments of the deep sea, *Global Biogeochem. Cycles*, 10(1), 158–159, 1996.
- Archer, D., and E. Maier-Reimer, Effect of deep-sea sedimentary calcite preservation on atmospheric CO<sub>2</sub> concentration, *Nature*, 367, 260–263, 1994.
- Archer, D., D. Lea, and N. Mahowald, What caused the glacial/interglacial atmospheric pCO<sub>2</sub> cycles?, *Rev. Geophys.*, 38, 159–189, 2000.
- Aumont, O., Étude du cycle naturel du carbone dans un modèle 3D de l'océan mondial, Doctorat thesis, Univ. Pierre et Marie Curie, Paris, 1998.
- Bacastow, R. B., and E. Maier-Reimer, Ocean-circulation model of the carbon cycle, *Clim. Dyn.*, 4, 95–125, 1990.
- Balch, W. M., and K. Kilpatrick, Calcification rates in the equatorial Pacific along 140°W, *Deep Sea Res., Part II*, 43, 971–993, 1996.
- Balch, W. M., D. T. Drapeau, and J. J. Fritz, Monsoonal forcing of calcification in the Arabian Sea, *Deep Sea Res., Part II*, 47, 1301–1337, 2000.
- Bates, N. R., Interannual variability of oceanic CO<sub>2</sub> and biogeochemical properties in the Western North Atlantic subtropical gyre, *Deep Sea Res., Part II*, 48, 1507–1528, 2001.
- Bates, N. R., A. F. Michaels, and A. H. Knap, Seasonal and interannual variability of the oceanic carbon dioxide system at the U. S. JGOFS Bermuda Atlantic time-series study site, *Deep Sea Res., Part II*, 43, 347–383, 1996.
- Bates, N. R., D. A. Hansell, and C. A. Carlson, Distribution of CO<sub>2</sub> species, estimates of net community production and air-sea exchange in the Ross sea polynya, *J. Geophys. Res.*, 103, 2883–2896, 1998.
- Bishop, J. K. B., Regional extremes in particulate matter composition and flux: Effects on the chemistry of the ocean interior, in *Productivity of the Ocean Present and Past*, edited by W. H. Broecker, V. S. Smetacek, and G. Wefer, pp. 117–137, John Wiley, New York, 1989.
- Brewer, P. G., G. T. F. Wong, M. P. Bacon, and D. W. Spencer, An oceanic calcium problem?, *Earth Planet. Sci. Lett.*, 26, 81–87, 1975.
- Broecker, W. S., Calcite accumulation rates and glacial to interglacial changes in oceanic mixing, in *The Late Cenozoic Glacial Ages*, edited by K. K. Turekian, pp. 239–265, Yale Univ. Press, New Haven, Conn., 1971.
- Broecker, W. S., and T.-H. Peng, *Tracers in the Sea*, 690 pp., Lamont-Doherty Geol. Obs., Palisades, N. Y., 1982.
- Brown, C. W., and J. A. Yoder, Coccolithophorid blooms in the global ocean, *J. Geophys. Res.*, 99, 7467–7482, 1994.
- Buesseler, K. O., Do upper-ocean sediment traps provides an accurate record of particle flux?, *Nature*, 353, 420–4423, 1991.
- Chipman, D. W., and T. Takahashi, Investigation of carbon chemistry in the Weddell Sea area during the 1986 winter expedition of the F/S Polarstern, report, Lamont-Doherty Geol. Obs., Palisades, N. Y., 1986.
- Chipman, D. W., T. Takahashi, D. Breger, and S. C. Sutherland, Carbon dioxide, hydrographic, and chemical data obtained during the R/V *Meteor* cruise 11/5 in the South Atlantic and northern Weddell Sea (WOCE Sections A-12 and A-21), report, 50 pp., Carbon Dioxide Inf. Anal. Cent., Oak Ridge Natl. Lab., Oak Ridge, Tenn., 1994.
- Deutsch, C., N. Gruber, R. M. Key, and J. L. Sarmiento, Denitrification and N<sub>2</sub> fixation in the Pacific Ocean, *Global Biogeochem. Cycles*, 15(2), 483–506, 2001.
- Dickson, A. G., and F. J. Millero, A Comparison of the equilibrium constants for the dissociation of carbonic acid in seawater media, *Deep Sea Res.*, 34, 1733–1743, 1987.
- Fabry, V. J., Aragonite production by pteropod molluscs in the subarctic Pacific, *Deep Sea Res.*, 36, 1735–1751, 1989.
- Fernández, E., P. Boyd, P. M. Holligan, and D. S. Harbour, Production of organic and inorganic carbon within, *Mar. Ecol. Prog. Ser.*, 97, 271–285, 1993.
- Ganachaud, A. S., Large scale oceanic circulation and fluxes of freshwater, heat, nutrients and oxygen, Ph.D., thesis, Mass. Inst. of Technol. and the Woods Hole Oceanogr. Inst., Cambridge, Mass., 1999.
- Gnanadesikan, A., R. D. Slater, N. Gruber, and J. L. Sarmiento, Oceanic vertical exchange and new production: A comparison between models and observations, *Deep Sea Res., Part II*, 49, 363–401, 2002.
- Gruber, N., and J. L. Sarmiento, Global patterns of marine nitrogen fixation and denitrification, *Global Biogeochem. Cycles*, 11(2), 235–266, 1997.
- Hernes, P. J., M. L. Peterson, J. W. Murray, S. G. Wakeham, C. Lee, and J. I. Hedges, Particulate carbon and nitrogen fluxes and compositions in the central equatorial Pacific, *Deep Sea Res., Part I*, 48, 1999–2023, 2001.
- Holligan, P. M., et al., A biogeochemical study of the coccolithophore, *Emiliania huxleyi*, in the North Atlantic, *Global Biogeochem. Cycles*, 7(4), 879–900, 1993.
- Honjo, S., Fluxes of particles to the interior of the open oceans, in *Particle Flux in the Ocean*, edited by V. Ittekkot, et al., pp. 91–154, John Wiley, New York, 1996.
- Iglesias-Rodríguez, M. D., C. Brown, S. C. Doney, J. Kleypas, D. Kolber, Z. Kolber, P. K. Hayes, and P. G. Falkowski, Representing key phytoplankton functional groups in ocean carbon cycle models: Coccolithophores, *Global Biogeochem. Cycles*, 16, doi:10.1029/2001GB001454, in press, 2002.
- Johnson, K. M., B. Schneider, L. Mintrop, and D. W. R. Wallace, Carbon dioxide, hydrographic, and chemical data obtained during the R/V *Meteor* cruise 18/1 in the North Atlantic Ocean (WOCE Section A1E, September 1991), report, 53 pp., Carbon Dioxide Inf. Anal. Cent., Oak Ridge Natl. Lab., Oak Ridge, Tenn., 1996.
- Karl, D., R. Letelier, L. Tupas, J. Dore, J. Christian, and D. Hebel, The role of nitrogen fixation in biogeochemical cycling in the subtropical North Pacific Ocean, *Nature*, 388, 533–588, 1997.
- Kortzinger, A., W. Koeve, P. Kahler, and L. Mintrop, C:N ratios in the mixed layer during the productive season in the northwest Atlantic Ocean, *Deep Sea Res., Part I*, 48, 661–687, 2001.
- Lamb, M. F., et al., Consistency and synthesis of Pacific Ocean CO<sub>2</sub> survey data, *Deep Sea Res., Part II*, 49, 21–58, 2002.
- Laws, E. A., P. G. Falkowski, W. O. Smith Jr., H. Ducklow, and J. J. McCarthy, Temperature effects on export production in the open ocean, *Global Biogeochem. Cycles*, 14(4), 1231–1246, 2000.
- Lee, K., Global net community production estimated from the annual cycle of surface water total dissolved inorganic carbon, *Limnol. Oceanogr.*, 46, 1287–1297, 2001.
- Li, Y. H., T. Takahashi, and W. S. Broecker, Degree of saturation of CaCO<sub>3</sub> in the oceans, *J. Geophys. Res.*, 74, 5507–5525, 1969.
- Maier-Reimer, E., Geochemical cycles in an ocean general circulation model, Preindustrial tracer distributions, *Global Biogeochem. Cycles*, 7(3), 645–677, 1993.
- Martin, J. H., G. A. Knauer, D. M. Karl, and W. W. Broenkow, VERTEX: Carbon cycling in the northeast Pacific, *Deep Sea Res.*, 34, 267–285, 1987.
- Matsumoto, K., J. L. Sarmiento, and M. A. Brzezinski, Silicic acid leakage from the Southern Ocean as a possible mechanism for explaining glacial atmospheric pCO<sub>2</sub>, *Global Biogeochem. Cycles*, 16(3), 1031, 10.1029/2001GB001442, 2002.
- Mehrbach, C., C. H. Culbertson, J. E. Hawley, and R. M. Pytkowicz, Measurement of the apparent dissociation constants of carbonic acid in seawater at atmospheric pressure, *Limnol. Oceanogr.*, 18, 897–907, 1973.
- Millero, F. J., S. Fiol, D. M. Campbell, G. Parrilla, L. J. Allison, and A. Kozyr, Carbon dioxide, hydrographic, and chemical data obtained during the R/V *Hespérides* cruise in the Atlantic Ocean (WOCE Section A5, July 14–August 15, 1992), report, 51 pp., Carbon Dioxide Inf. Anal. Cent., Oak Ridge Natl. Lab., Oak Ridge, Tenn., 2000.
- Milliman, J. D., Production and accumulation of calcium carbonate in the ocean: Budget of a nonsteady state, *Global Biogeochem. Cycles*, 7(4), 927–957, 1993.
- Milliman, J. D., and P. J. Troy, Biologically mediated dissolution of calcium carbonate above the chemical lysocline?, *Deep Sea Res., Part I*, 46, 1653–1670, 1999.

- Minster, J.-F., and M. Boulahdid, Redfield ratios along isopycnal surfaces—A complementary study, *Deep Sea Res.*, *34*, 1981–2003, 1987.
- Murnane, R., J. L. Sarmiento, and C. L. Quéré, Spatial distribution of air-sea CO<sub>2</sub> fluxes and the interhemispheric transport of carbon by the oceans, *Global Biogeochem. Cycles*, *13*(2), 287–305, 1999.
- Murray, J. W., J. Young, J. Newton, J. Dunne, T. Chapin, B. Paul, and J. J. McCarthy, Export flux of particulate organic carbon from the central equatorial Pacific determined using a combined drifting trap-<sup>234</sup>Th approach, *Deep Sea Res., Part II*, *43*, 1095–1132, 1996.
- Oceanographic Data Facility, Physical, chemical and in situ CTD data from the AJAX expedition in the south Atlantic Ocean, report, 275 pp., Scripps Inst. of Oceanogr., Univ. of Calif., San Diego, La Jolla, 1985.
- Oceanographic Data Facility, HYDROS Leg 4, 190 pp., report, Scripps Inst. of Oceanogr., Univ. of Calif., San Diego, La Jolla, 1992a.
- Oceanographic Data Facility, South Atlantic Ventilation Experiment (SAVE) chemical, physical and CTD data report Legs 1–3, report, 729 pp., Scripps Inst. of Oceanogr., Univ. of Calif., San Diego, La Jolla, 1992b.
- Oceanographic Data Facility, South Atlantic Ventilation Experiment (SAVE) chemical, physical and CTD data report Legs 4–5, report, 625 pp., Scripps Inst. of Oceanogr., Univ. of Calif., San Diego, La Jolla, 1992c.
- Redfield, A. C., B. H. Ketchum, and F. A. Richards, The influence of organisms on the composition of seawater, in *The Sea*, edited by M. N. Hill, pp. 26–77B, Wiley-Interscience, New York, 1963.
- Rintoul, S. R., and C. Wunsch, Mass, heat, oxygen and nutrient fluxes and budgets in the North Atlantic Ocean, *Deep Sea Res.*, *38*, Suppl. 1, S355–S377, 1991.
- Robertson, J. E., C. Robinson, D. R. Turner, P. Holligan, A. J. Watson, P. Boyd, E. Fernandez, and M. Finch, The impact of a coccolithophore bloom on oceanic carbon uptake in the northeast Atlantic during summer 1991, *Deep Sea Res., Part I*, *41*, 297–314, 1994.
- Rodier, M., and R. Le Borgne, Export of particles at the equator in the western and central Pacific Ocean, *Deep Sea Res., Part II*, *44*, 2085–2113, 1997.
- Rubin, S. I., T. Takahashi, D. W. Chipman, and J. G. Goddard, Primary productivity and nutrient utilization ratios in the Pacific sector of the Southern Ocean based on seasonal changes in seawater chemistry, *Deep Sea Res., Part I*, *45*, 1211–1234, 1998.
- Sabine, C. L., R. M. Key, K. M. Johnson, F. J. Millero, A. Poisson, J. L. Sarmiento, D. W. R. Wallace, and C. D. Winn, Anthropogenic CO<sub>2</sub> inventory of the Indian Ocean, *Global Biogeochem. Cycles*, *13*(1), 179–198, 1999.
- Sabine, C. L., H. W. Feely, R. M. Key, J. L. Bullister, F. J. Millero, K. Lee, T.-H. Peng, B. Tilbrook, T. Ono, and C. S. Wong, Distribution of anthropogenic CO<sub>2</sub> in the Pacific Ocean, *Global Biogeochem. Cycles*, *16*, doi:10.1029/2001GB001629, in press, 2002.
- Sarmiento, J. L., P. Monfray, E. Maier-Reimer, O. Aumont, R. Murnane, and J. Orr, Air-sea CO<sub>2</sub> fluxes and carbon transport: A comparison of three ocean general circulation models, *Global Biogeochem. Cycles*, *14*(4), 1267–1281, 2000.
- Shaffer, G., J. Bendsen, and O. Ulloa, Fractionation during remineralization of organic matter in the ocean, *Deep Sea Res., Part I*, *46*, 185–204, 1999.
- Sundquist, E. T., Geological perspectives on carbon dioxide and the carbon cycle, in *The Carbon Cycle and Atmospheric CO<sub>2</sub>: Natural Variations Archean to Present*, *Geophys. Monogr. Ser.*, vol. 32, edited by E. T. Sundquist, and W. S. Broecker, pp. 5–59, AGU, Washington, D. C., 1985.
- Sweeney, C., D. A. Hansell, C. A. Carlson, L. A. Codispoti, L. I. Gordon, J. Marra, F. J. Millero, W. O. Smith, and T. Takahashi, Biogeochemical regimes, net community production and carbon export in the Ross Sea, Antarctica, *Deep Sea Res., Part II*, *47*, 3369–3394, 2000.
- Takahashi, T., C. Goyet, D. Chipman, E. Peltzer, J. Goddard, and P. G. Brewer, Ratio of the organic carbon and calcium carbonate productions observed at the JGOFS 47°N–20°W site, in *Joint Global Ocean Flux Study, North Atlantic Bloom Experiment, Int. Sci. Symp., JGOFS Rep. 7*, pp. 76–77, Sci. Comm. on Oceanic Res., Washington, D.C., 1990.
- Tsunogai, S., and S. Noriki, Particles fluxes of carbon and organic carbon in the ocean: Is the marine biological activity working as a sink of the atmospheric carbon?, *Tellus, Ser. B*, *43*(2), 256–266, 1991.
- Wanninkhof, R., R. A. Feely, D. K. Atwood, G. Berberian, D. Wilson, P. P. Murphy, and M. F. Lamb, Seasonal and lateral variations in carbon chemistry of surface water in the eastern equatorial Pacific during 1992, *Deep Sea Res., Part II*, *42*, 387–409, 1995.
- Yamanaka, Y., and E. Tajika, The role of the vertical fluxes of particulate organic matter and calcite in the ocean carbon cycle: Studies using an ocean biogeochemical general circulation model, *Global Biogeochem. Cycles*, *10*(2), 361–382, 1996.
- Ziveri, P., A. T. C. Broerse, J. E. van Hinte, P. Westbroek, and S. Honjo, The fate of coccoliths at 48°N 21°W, northeastern Atlantic, *Deep Sea Res., Part II*, *47*, 1853–1875, 2000.

J. Dunne, R. M. Key, K. Matsumoto, J. L. Sarmiento, and R. Slater, Atmospheric and Oceanic Sciences Program, Princeton University, Sayre Hall, Forrester Campus, P.O. Box CN710, Princeton, NJ 08544-0710, USA. (jdunne@splash.princeton.edu; key@princeton.edu; kmatsumo@splash.princeton.edu; jls@princeton.edu; rdslater@splash.princeton.edu)

A. Gnanadesikan, Geophysical Fluid Dynamics Laboratory, NOAA, Princeton University, P.O. Box 308, Princeton, NJ 08542, USA. (gnana@splash.princeton.edu)